SOLVENT-FREE, LIQUID PROCESSABLE BT RESIN/GLASS FIBRE REINFORCED COMPOSITES

Robert J. Iredale[1] and Ian Hamerton[1]

[1]Bristol Composites Institute (ACCIS), Department of Aerospace Engineering, School of Civil, Aerospace, and Mechanical Engineering, Queen's Building, University Walk, University of Bristol, Bristol, BS8 1TR, U.K.
Email: robert.iredale@bristol.ac.uk

Keywords: Bismaleimide, Cyanate Ester, Thermoset, Resin infusion

Abstract
Bismaleimide-triazine (BT) resins are a class of high performance thermoset matrices that has historically suffered from poor processability. In this work, a novel BT resin is successfully utilised to produce woven glass composite laminates using a room temperature, vacuum-assisted resin infusion technique. The suitability of the first step of the cure cycle to composite manufacture is validated using isothermal dynamic scanning calorimetry. An initial dwell period at 170 °C for two hours facilitates sufficient conversion to enable the use of industry standard consumables, negating the need for more expensive materials and tooling. Fibres with three different surface treatments (unsized, aminosilane-, and Volan™-functionalised) are compared in terms of processability, and mechanical and temperature performance. Volan™-functionalised fibre composites are found to exhibit superior mechanical performance, with a short beam shear strength of 65 MPa and a storage modulus of 7.93 GPa. The different sizings also lead to variations in temperature performance, with changes to the behaviour around the glass transition temperature evident between the different composite plates.

1. Introduction

Bismaleimide-triazine (BT) resins possess a range of desirable characteristics including good mechanical performance, high glass transition temperature (T_g) and low dielectric constant and loss (D_k and D_f respectively) [1]. These properties arise thanks to the combination of two high performance resin systems, namely cyanate esters (CEs) and bismaleimides (BMIs), and make them suitable to both microelectronic and stealth applications [2]. However, BT resins have traditionally suffered from poor processability, requiring either high temperatures (>150 °C) or harmful, high boiling solvents to render them useful in composite manufacture. This issue has been addressed in a number of ways, such as by incorporating epoxies into the blend, utilizing lower viscosity monomers or by developing novel monomers with lower melting points [3-6]. Furthermore, BT resins that are processable at intermediate temperatures (90 °C) have been demonstrated, however these blends exhibit poorer electrical performance [7]. A novel liquid processable BT resin blend, designated LPBT, has been developed in-house with the aim of imparting low temperature infusibility to a BT system. Using commercial monomers as its constituent parts, it exhibits lower viscosities and contains less toxic monomers than industrial standards. A summary of some of the advantageous properties of this blend are found in Figure 1 and Table 1.

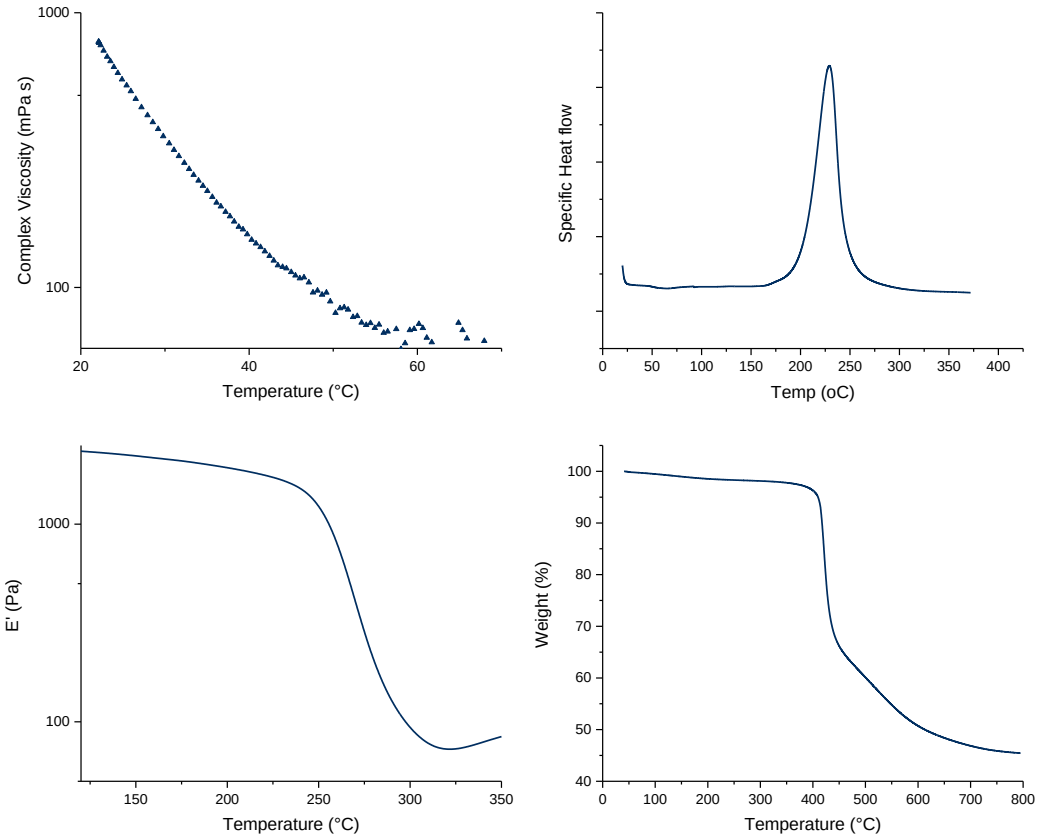

Figure 1. Selected physical data displaying the interesting features of the LPBT resin, including rheology (top left), differential scanning calorimetry (top right), dynamic mechanical analysis (bottom left) and thermogravimetric analysis (bottom right) plots.

Table 1. Summary of resin properties for the LPBT resin.

Property	Value	Units	Notes
Viscosity at 30 °C	260	mPa s	
Gel temperature	212	°C	5°C min^{-1} ramp rate
Processing window	> 100	°C	
Dielectric constant	2.95	-	
T_g	280	°C	tan δ peak

This work investigates the next step in the development of this resin system, assessing whether its apparent beneficial properties can be translated into an industrially useful composite. The low-temperature infusibility of LPBT will be investigated, whilst simultaneously evaluating the performance of fibres with different surface treatments in combination with a BT resin. Selecting the appropriate fibre surface treatment is extremely important to both the manufacturing and performance aspects of a composite material. There is little evidence in the literature of investigations into the effect of fibre sizing on the properties BT resin composites. One study showed that introducing a polyethylene glycol layer to the surface of the glass results in increased toughness and strength, at the cost of reductions in stiffness and temperature performance [8]. Other studies have only dealt with either the BMI or CE component individually [9, 10].

Three different glass fibre treatments were assessed for use with the LPBT resin: unsized fibres, amino functionalised fibres, and methacrylate functionalised fibres (herein designated as GF_{un}, GF_{am} and GF_{vol}, respectively). The amino sizing is based upon a traditional silane treatment, whereas the methacrylate-sizing involves a Volan™ coupling agent, with the chemical structures of their building blocks displayed in Figure 2.

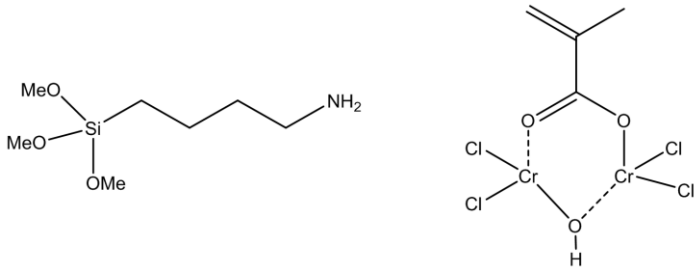

Figure 2. Chemical structures of the aminosilane and Volan™ surface treatments.

Both of these treatments can be expected to interact with the resin in different ways. In the case of the Volan™ fibres, the double bond containing methacrylate group is able to undergo free radical polymerisation with the bismaleimide (BMI) monomers, thereby forming chemical crosslinks with the resin. The cyanate ester component does not react with this functional group, but the complex might be expected to improve composite properties in a different way: catalysis. It is well known that transition metal co-ordination complexes, in this instance with Cr^{3+} as the metal ion, are efficient catalysts for the polymerisation of cyanate ester monomers [11 ,12]. However, this catalysis route depends upon the availability of co-ordination sites on the metal centre, which may be sterically hindered in the sizing layer. Therefore, any potential catalysis benefits will need to be tested experimentally. The silane functionalised fibres contain readily available, nucleophilic primary amine groups. These can be expected to react with both resin constituents in different ways. Amines are well known to co-react with BMIs *via* a rapid Michael addition reaction to yield a saturated aspartimide ring in the reaction scheme outlined in Figure 3 [13].

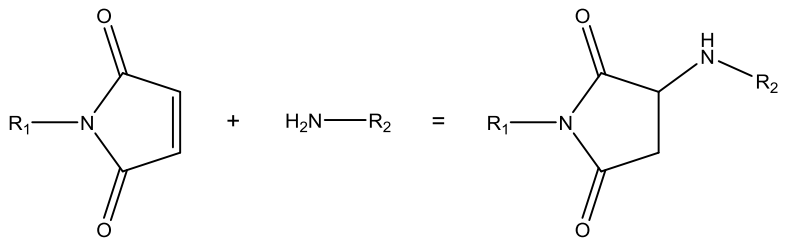

Figure 3. The reaction between a maleimide and an amine.

Similarly, cyanate esters are susceptible to nucleophilic attack from both primary and secondary amines [14, 15], forming isourea ethers according to Figure 4.

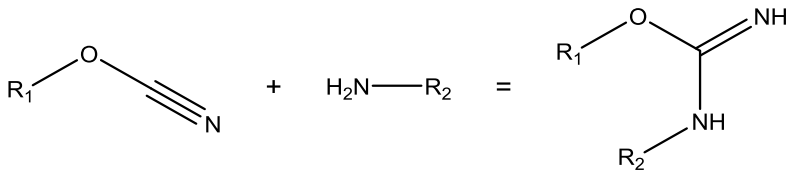

Figure 4. The reaction between a cyanate ester and an amine.

It is therefore possible that this treatment might lead to strong interfacial bonding between fibre and matrix. However, the competitiveness of these reactions with the standard homopolymerisation of the monomers remains to be seen.

The surfaces of the unsized fibres are likely to contain numerous hydroxyl moieties, which can also act as weak nucleophiles. However, these groups are much weaker nucleophiles and the functional groups are sterically hindered, due to their proximity to the fibre surface. It is therefore expected that composites made using these fibres will exhibit the poorest performance.

2. Experimental

2.1. Materials

Resin components were either purchased from Lonza AG or supplied by Evonik Industries and used as received. Glass fibre samples with different surface treatments were provided by Fothergill Engineered Fabrics.

2.2. Differential scanning calorimetry

Dynamic scanning calorimetry (DSC) experiments were performed on uncured resin samples using a TA DSC Q2000 machine. Hermetically sealed Tzero aluminium pans were used, with sample masses of 12 ± 2 mg and an empty pan as the reference. The cell was heated to the desired isothermal temperature, at which point the sample pan was inserted and the experiment was started. The sample cell was kept under a constant nitrogen flow of 50 cm^3 min^{-1}.

2.3. Plate manufacture

Composite specimens were prepared using a vacuum-assisted resin infusion technique, with the aim of introducing the resin under ambient conditions before curing at elevated temperatures. Glass fibre preforms, consisting of 20 woven glass layers with dimensions 110 x 80 mm^2, were cut and laid up by hand. A vacuum bagging setup was prepared as outlined in Figure 5, with all of the preforms located in the same bag.

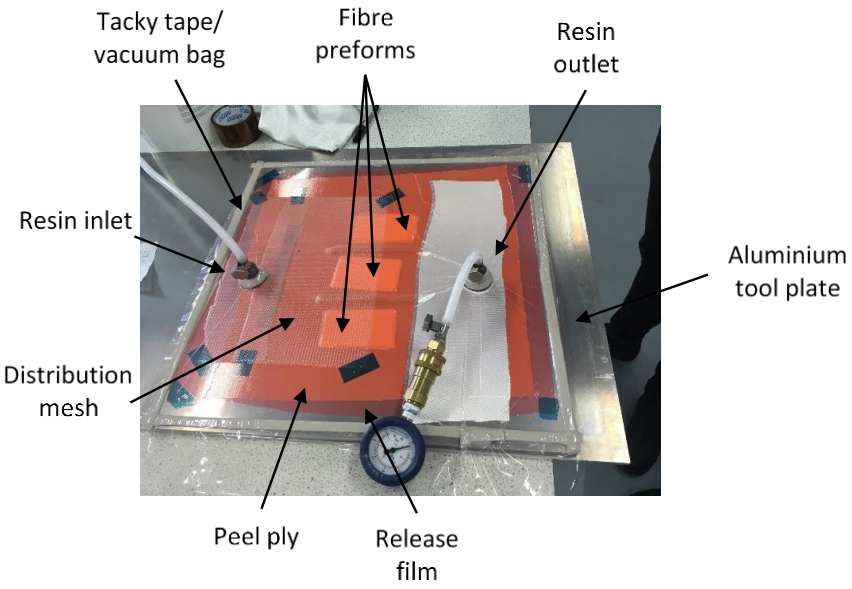

Figure 5. Photograph of the vacuum infusion setup used during composite manufacture.

The infusion set-up is designed in such a way that each laminate is subjected to identical conditions (resin blend, pressure, and temperature) and therefore the processing variability between the different plates is minimized. A vacuum pump was then used to pull the pre-mixed resin through the fibres, with the outlet sealed with a clamp once the resin had emerged from the valve. A regular composite vacuum bag was then applied over the top of the initial bag in order to apply consolidating pressure over the laminate during cure. The plates were oven cured under vacuum pressure at 170 °C for 2 hours, before being removed from the bag. A free standing post-cure with the following temperature dwells was then applied: 200 °C (4 hours), 220 °C (2 hours), and 250 °C (4 hours).

2.4. Mechanical testing

Short beam shear testing was undertaken according to ASTM D2344, with the aim of inducing interlaminar shear failure and using the determined critical stress as a measure of the interface strength between the fibres and the matrix. The thickness of the specimens was measured to be 3.3 ± 2 mm, with the rest of the sample dimensions cut accordingly (width = 2 x thickness, length = 6 x thickness). The specimens were then tested in three-point bending.

The short beam shear strength (F^{sbs}) was then calculated according to the equation (Eq. 1),

$$F^{sbs}=3P_m/4bh\ , \tag{1}$$

where P_m is the maximum load reached during the test and b and h are the measured specimen width and thickness respectively. In each case, a failure type is reported, as this method of testing can lead to failure modes other than ILSS (particularly tensile or compressive failures).

2.5. Scanning electron microscopy

Scanning electron microscopy (SEM) images were taken using a Hitachi TM3030Plus SEM unit, at an accelerating voltage of 15 kV. Samples were sputter coated with a 20 nm thick layer of silver prior to imaging.

2.6. Dynamic mechanical thermal analysis

Dynamic mechanical thermal analysis (DMTA) measurements were performed using a TA DMA Q800 instrument equipped with a single cantilever bending fixture. Sample dimensions of the bars were 3.3 x 7 x 35 mm^3, with a displacement amplitude of 15 μm, frequency of 1 Hz and temperature ramp rate of 5 °C min^{-1} used throughout.

3. Results and discussion

3.1 Cure cycle validation

The aim of the initial experiment was to prove and assess the infusibility of the resin system while evaluating the processing and performance aspects of each of the different glass fibres. The move from neat resin to composite material invokes a number of additional considerations that must be taken into account, particularly where the cure cycle is concerned. Commercial BT resin systems typically involve high temperature cure steps, which can be prohibitive for conventional bagging and tooling materials. The maximum use temperature of these components can be increased, but often at high financial cost. Therefore, it is important that the cure cycle can be modified in such a way that widely used consumables can still be employed, specifically enabling vitrification at temperatures lower than 180 °C. Isothermal DSC measurements were used to assess appropriate initial cure temperatures and dwell times for the neat resin. Thus, experiments were performed at 160 °C, 170 °C, 180 °C, and 200 °C, with the results in terms of both heat flow and conversion displayed in Figure 6 and key points are summarised in Table 2. The conversion, or degree of cure, of the resin (α) is calculated according to the equation (Eq. 2),

$$\alpha = \Delta H_t / \Delta H_T , \quad (2)$$

where ΔH_t is the cure enthalpy change at time t and ΔH_T is the total enthalpy of cure for the blend (calculated from a dynamic DSC measurement, with a heating rate of 10 °C min^{-1}, to be 578 J g^{-1}).

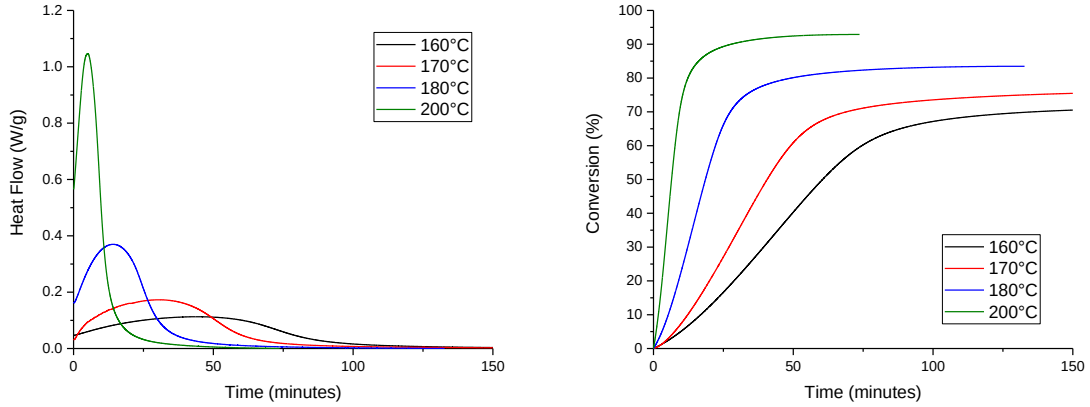

Figure 6. Plots of heat flow (left) and conversion (right) against time from the isothermal DSC experiments.

Table 2. Summary of key points from isothermal DSC experiment.

Isothermal temperature (°C)	$t_{\Delta H_{max}}$ [1] (mins)	$t_{\alpha_{95\%}}$ [2] (mins)	α_{max} [3] (%)
160	43	105	71
170	30	96	76
180	14	45	83
200	5	22	93

[1] $t_{\Delta H max}$ is the time at which maximum heat flow is reached. [2] $t_{\alpha 95\%}$ is the time taken to reach 95 % conversion at a given temperature (α_{max} x 0.95). [3] α_{max} is the maximum conversion reached.

The heat flow curves follow the expected shape, with a parabolic peak tending towards a constant value. This results in conversion plots that start with a steep gradient before tending towards the maximum conversion value possible at the corresponding temperature. The time taken to reach peak heat flow, analogous to gel time, decreases drastically as the temperature is raised. Furthermore, the maximum value of heat flow significantly increases with temperature, ultimately resulting in higher conversions at higher temperatures. The recommended cure cycle for two of the components of the resin blend involves an initial dwell at 170 °C for 2 hours. The data presented here show that this will lead to a degree of cure of around 70 %, which will result in vitrified samples than can readily be removed from the bagging materials and will be able to withstand free standing post cure without warping or creeping under gravity. This first step is therefore deemed appropriate for composite preparation using this resin blend, with the specimens being removed from the bagging materials after this initial dwell period.

3.2 Resin infusion

While the interface between the fibre and resin is important for optimizing composite properties, other factors such as fibre formability and permeability are often overlooked in studies regarding sizing effects. This can be particularly true for infusion, where dry fabrics are utilized. The fibres used in this study showed a clear manufacturability difference during the lay-up phase of the plate preparation. The unsized fibres (GF_{un}) were problematic to handle, with the fibres crimping and becoming easily misaligned when plies were laid on top of one another. This issue was further exacerbated once vacuum was applied, causing the plies to slip over one another resulting in large overlaps. This will lead to drop offs in the mechanical performance of the composite. Conversely, the GF_{am} fibres were much easier to handle, maintaining their shape when cut into plies and laid up. The sizing appeared to increase the stiffness of the fibre tows preventing deformation. There is a chance that this increased stiffness might actually reduce the conformability of the fabric for more complex shapes than the flat panels used here. The GF_{vol} fibres represented a middle ground in terms of ease of handling, compared to the other fibre types used in this study.

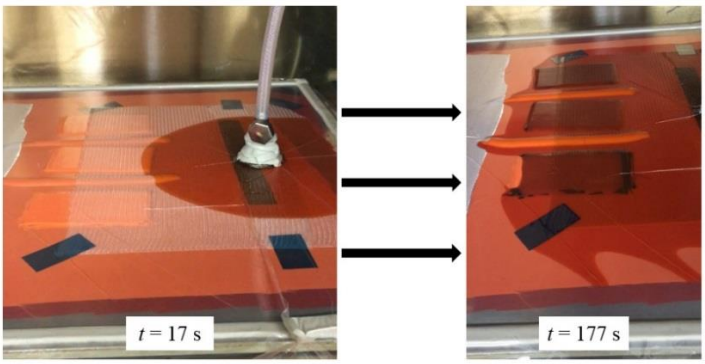

Figure 7. Photographs showing infusion progression at different stages of the experiment.

The room temperature vacuum infusion of the panels was successful, with the resin having fully progressed through the fibres of all three plates in less than five minutes. The resin was drawn through the entire vacuum bag before the system was sealed: this technique was implemented in order to prevent any bleed out issues once the resin viscosity drops as the temperature is raised. Images of the process are displayed in Figure 7. After the initial cure at 170 °C the plates had vitrified, enabling their removal from the bagging. After post curing, all three plates attained a dark brown colour characteristic of the neat LPBT resin samples. A resin burn off experiment at 600 °C was used to assess the composition of the samples: each plate yielded a fibre weight fraction of 60 %, which was extrapolated to give an approximate fibre volume fraction of 43 %, with the values being consistent for all three samples. While these volume fractions are lower than those attainable through autoclave processing, they were deemed acceptable here thanks to the lower pressure capabilities of the fabrication method and lack of control over inlet resin volume. These plates were then cut using a diamond saw before being subjected to mechanical testing.

3.3 Short beam shear testing

Representative plots of the raw data recorded by the machine for each fibre type are displayed in Figure 8. Immediately evident is the marked difference in peak load attained by each specimen, with variations in the order of 400 N between the fibre types. The load-extension curves also reveal differences in failure mechanisms occurring, corresponding to the differences seen during testing. The GF_{un} composites fail in an incremental fashion, with small drop-offs in load. This might indicate a layer by layer failure of the material, and similarly represent poor stress transfer across the interlaminar regions. Conversely, the GF_{am} specimens fail catastrophically, with a sharp loss of load-bearing capability (the load drops by over 30%) upon failure. Similar, behaviour is seen for the GF_{vol} composites, albeit with more significant load retention.

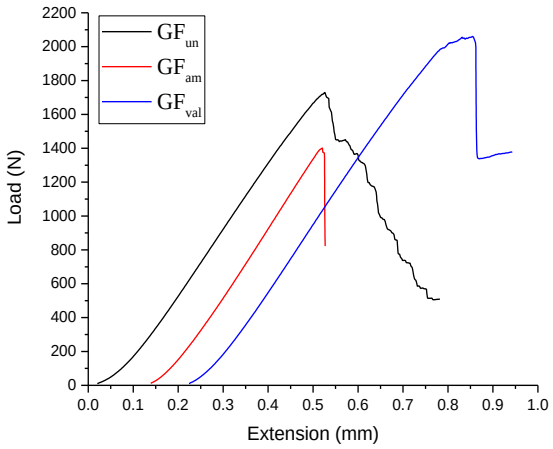

Figure 8. Examples of raw data plots obtained or the short beam shear tests of the different laminates. Extensions are offset for clarity.

The results were then processed according to Equation 1. F^{sbs} values obtained for each of the composite specimens are displayed in Table 3, along with additional notes related to the test. The standard deviations for all the fibre types are small, suggesting excellent reproducibility and homogeneity of the composites. This is important in showing the success of the infusion process, as any defects or inhomogeneity would appear as outliers in this data set.

Table 3. Summary of findings of the short beam shear experiment.

Fibre type	F^{sbs} (MPa)	Failure type	Notes
GF_{un}	54 ± 2	Tensile - incremental	Difficult to handle
GF_{am}	45 ± 3	Tensile - sudden	Poor infusion quality
GF_{vol}	65 ± 2	Mixed ILSS/Tensile	-

The results show that the combination of LPBT resin with GF_{vol} fibres yields vastly superior mechanical performance to those produced through silane-based functionalization (GF_{am}) and unsized fibres (GF_{un}). F^{sbs} for the GF_{vol} composite is determined to be 65 MPa, over 10 MPa higher than the other specimens used here and comparing favourably with literature values for similar woven glass composites [16]. When considering the values obtained in this a study, a number of factors need to be taken into account: the interaction between the fibre and the resin, the quality of the laminate produced, and the strength of the fibres themselves.

3.4 Scanning electron microscopy

Scanning electron microscopy (SEM) was used to confirm the different fracture mechanisms put forward from the mechanical tests. Fracture surfaces of the tested specimens were imaged for each fibre type, with representative images being shown in Figures 9 – 11. Three distinct modes of failure were revealed in this analysis.

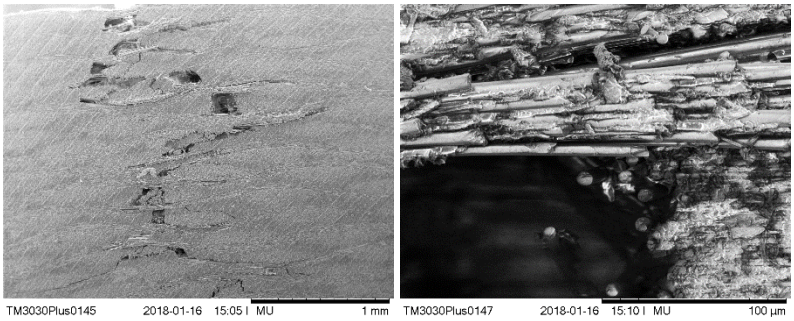

Figure 9. SEM images of GF_{un} fracture surfaces.

The images taken of the fractured GF_{un} based composites correspond very well with the incremental load drop-offs seen in the test. Within each layer of the composite there are cracks running perpendicular to the load direction, suggesting that each has failed progressively rather than a single crack running through sample. Furthermore, these cracks often run along the fibre resin interface, perhaps suggesting weak interaction between the two constituents. A further observation is that there appear to be a large number of broken fibres.

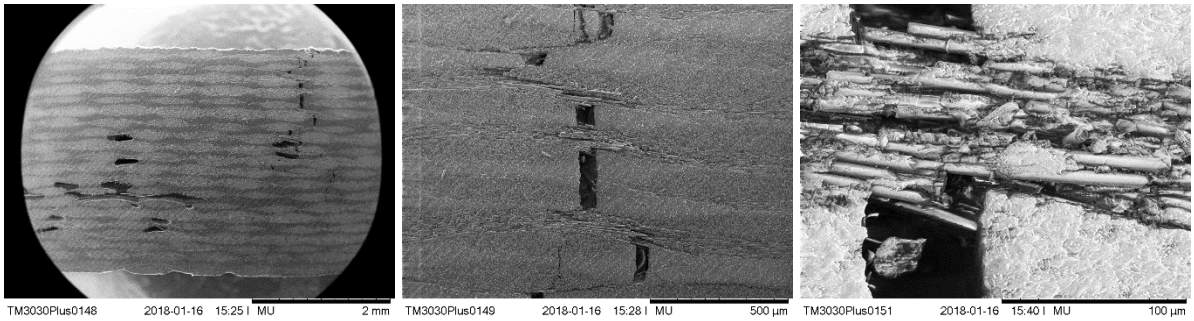

Figure 10. SEM images of GF_{am} fracture surfaces.

The first observation for the GF_{am} fibres is that there are numerous voids present in the sample, as evidenced by the dark, elliptical shapes on the cut surface of the specimen. While these are visible to the naked eye, the SEM images highlight the severity, and number of voids within the material. This shows that the sizing has impacted negatively upon the processing characteristics of the fibres, preventing complete permeation and wet out, ultimately resulting in reduced performance compared to even the unsized fibres (GF_{un}). It appears that sample failure has initiated at a stress concentration caused by the presence of one of these voids almost directly in line with the loading head. The crack propagates through the interlaminar regions parallel to the loading direction, jumping along the fibre when it reaches the longitudinal layers. This implies further poor impregnation amongst the fibres, as the crack readily runs through the fibre layers unhindered, seemingly without causing significant damage to the fibres themselves as they remain bridged across the crack.

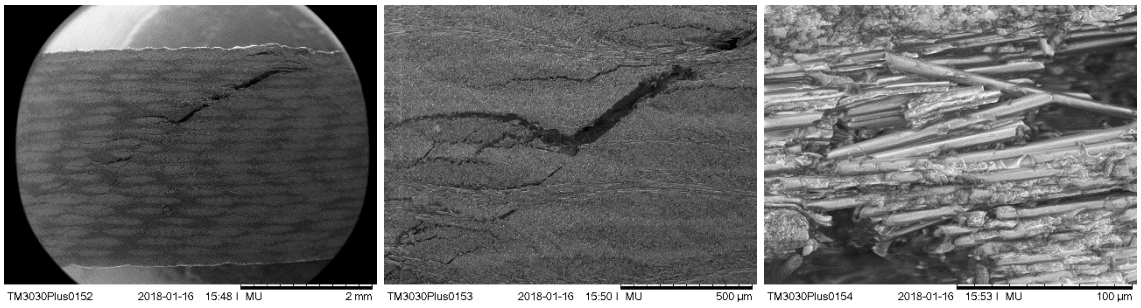

Figure 11. SEM images of GF_{vol} fracture surfaces.

The SEM images of the GF_{vol} specimens confirm the observation of a third, different fracture mechanism. Here, the crack initiates in an interlaminar shear type mechanism, with the start of the crack parallel to the sample edge. It then proceeds to run diagonally through the material, in between the fibre tows. When the crack finally reaches a tow, it diverges into several small cracks that run both inter- and intra-tow. In this instance, it appears that the crack penetrates much further into the material than in the previous cases.

The images taken at high magnification do not reveal any significant difference between the different specimens. In each instance there appear to be bare fibre surfaces as well as tows impregnated with resin. Therefore, no additional information as to the interfacial strength between the resin and each fibre can be garnered from these images. In order to further understand the properties of these composites, microbond testing is required to directly measure the interfacial strength between fibre and matrix in each instance.

3.5 Dynamic mechanical thermal analysis

DMTA was used to analyse both thermal and mechanical properties of the composites produced. This technique enables any changes in stiffness or glass transition temperature (T_g) between the different specimens to be identified. The results from these analyses are displayed in Figure 12 and Table 4.

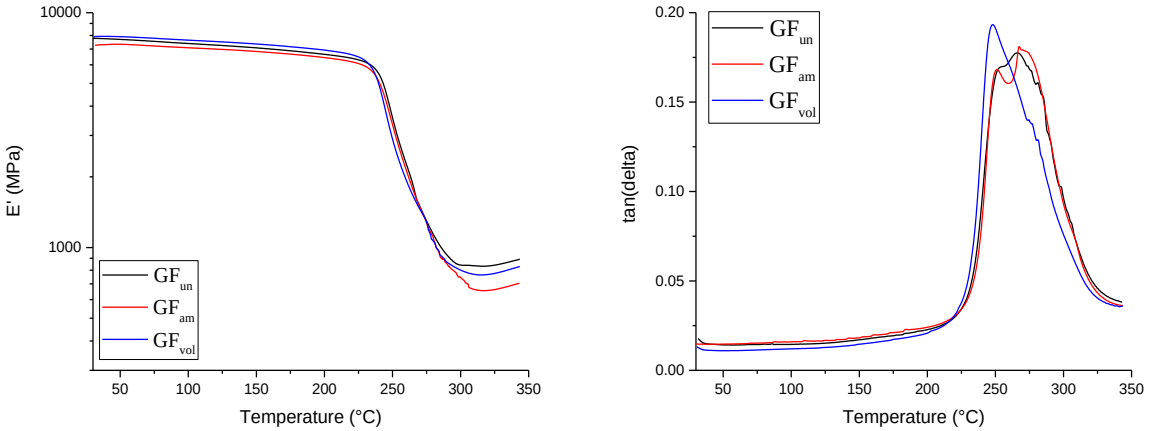

Figure 12. Plots of both storage modulus (E') and tan(δ) obtained from DMTA measurements performed on cured laminates.

Table 4. Summary of key features arising from DMTA. [1] Measured at 35 °C. [2] Onset of storage modulus decrease. [3] Peak of tan(δ)

Fibre type	*E'* (GPa) [1]	T_g (°C) [2]	T_g (°C) [3]
GF_{un}	7.76	240	270
GF_{am}	7.30	239	266
GF_{vol}	7.93	236	243

Interestingly, DMTA revealed some marked differences in the dynamic mechanical properties of the resin for the different fibre types. While the blend used was identical for all three composite specimens, the fibre sizing appears to have influenced the resin curing to such a degree that the behaviour around T_g is quite different. At lower temperatures, the GF_{am} specimen has lower stiffness than the other materials, which can be explained by the poorer infusion quality achievable and high void content present. This is also true when the resin reaches the rubbery phase, with the greatest storage modulus drop of any of materials. Of the other systems, the GF_{vol} sample is almost 20 MPa stiffer than the composite based on unsized fibres, perhaps as a result of improved interfacial properties. However, it is at higher temperatures that the behaviour becomes more varied. Similar properties are exhibited by both the GF_{un} and GF_{am} composites upon initial softening and as the material enters the rubbery plateau, with the tan(δ) curves overlapping one another almost exactly. The GF_{un} material shows two distinct peaks, with maxima at 251 and 271 °C, with the separate peaks being attributed to the two separate, but interpenetrating polymer networks, namely BMI and CE. This observation substantiates previously made claims that the two systems do not react with one another in the absence of deliberate catalysis [17]. In the case of GF_{am} composite, the two peaks have moved closer together, merging to the point that the lower temperature peak appears as a strong shoulder on the higher temperature one. The maxima of the peaks are shifted to 254 and 266 °C respectively. This phenomenon might have arisen thanks to the nucleophilic amine groups reacting into both thermoset networks, essentially tethering them together and bringing their behaviour closer to that of a single network with intermediate properties of each. The tan(δ) peaks are also of a similar height. The behaviour changes more significantly in the case of the

GF_{vol} specimens, where the double peak seen previously has completely merged into a single peak skewed towards lower temperatures. This suggests one of two things: either the fibre sizing has led to the formation of a copolymerised network, or that the properties of the higher temperature component of the resin have been compromised. The maximum here occurs at 248 °C, in at a slightly lower temperature than the smaller peak on the other tan(δ) plots. Overall, it appears that while the GF_{vol} fibres produce the best mechanically performing composites, the temperature performance is adversely affected. However, this T_g decrease is not catastrophic for application, as it is the onset of storage modulus decrease that is most useful in defining the operating temperature of the composite, and this value only varies by 4 °C between all of the samples.

4. Conclusions

This experiment has taken the novel LPBT resin through the next stage of its development towards application in composite materials with good temperature and electrical performance. The curing rate of the resin shows a strong dependence on temperature in the range of 160 - 200 °C, allowing for vitrification at temperatures below 180 °C, which is desirable for current composite manufacturing standards. The curing behavior of the system could be further modified using catalysts for either resin component, presenting the opportunity to lower cure temperatures even further. The resin appears to lend itself readily to the infusion of woven glass preforms thank to its low viscosity, however at present this process has only been carried out on small plates. Further development and validation of the resin will involve the production of bigger specimens and complex shapes. Different fibre surface treatments have been shown to lead to marked changes in the properties of the LPBT composites produced. In terms of processability and mechanical performance, GF_{vol} fibres outperformed the other fibre types. Therefore, these fibres would be the recommended substrate for the infusion of these resins. More work is required to establish the interfacial shear stress to determine how much of the property improvement is down to the interaction between the constituents, as well as to investigate more thoroughly the differences in high temperature characteristics caused by the sizings.

5. Acknowledgements

The authors thank Dr Tim Pohlman and Dr Sergey Evsyukov (Evonik Industries) for supplying the BMI monomers. This work was supported by the Engineering and Physical Sciences Research Council through the EPSRC Centre for Doctoral Training in Advanced Composites for Innovation and Science [grant number EP/L016028/1].

6. References

[1] R. Iredale, C. Ward and I. Hamerton. Modern advances in bismaleimide resin technology: A 21st century perspective on the chemistry of addition polyimides. *Progress in Polymer Science*, 69:1-21, 2017.

[2] J. Gotro and B. Appelt. Characterisation of a bis-maleimide triazine resin for multilayer printed circuit boards. *IBM Journal of Research Development*, 8:83-95, 1996.

[3] Z. Ren, Y. Cheng, L. Kong, T. Qi and F. Xiao. High glass transition temperature bismaleimide-triazine resins based on soluble amorphous bismaleimide monomer. *Journal of Applied Polymer science*, 133:42882, 2016.

[4] Z. Ren, Y. Cheng, L. Kong and F. Xiao, Preparation and characterization of soluble bismaleimide-triazine resins based on soluble amorphous bismaleimide monomer. *Journal of Applied Polymer Science*, 134:1-8, 2017.

[5] M. Gaku, K. Suzuki and K Nakamichi. Curable Resin Compositions of Cyanate Esters. US 4110364, 1978.

[6] A. Crawford, G. Vacalli, B. Howlin and I. Hamerton. Investigation of structure property relationships in liquid processible, solvent free, thermally stable bismaleimide-triazine (BT) resins. *Reactive and Functional Polymers*, 102:110-118, 2016.

[7] A. Gu. High performance bismaleimide/cyanate ester hybrid polymer networks with excellent dielectric properties. *Composites Science and Technology*, 99:1749-1755, 2006.

[8] X. Zeng, S. Yu, M. Lai, R. Sun and C. Wong. Tuning the mechanical properties of glass fiber-reinforced bismaleimide-triazine resin composites by constructing a flexible bridge at the interface. *Science and Technology of Advanced Materials*, 14:065001, 2013.

[9] S. Mallarino, J. Chailan and J. Vernet. Glass fibre sizing effect on dynamic mechanical properties of cyanate ester composites I. Single frequency investigations. *European Polymer Journal*, 41:1804-1811, 2005.

[10] J. Favre, M. Auvray and P. Cheneau-Henry. Fiber/matrix mechanical interaction in carbon fiber/bismaleimide model composites. *Polymer Composites*, 17:937-947, 1996.

[11] T. Fang and D. Shimp, Polycyanate Esters: Science and Applications. *Progress in Polymer Science,* 20:61-118, 1995;

[12] J.N. Hay, Chapter 6 in *Chemistry and Technology of Cyanate Ester Resins*, I Hamerton (Ed.), 1994, Blackie A&P: Glasgow, pp. 151-192.

[13] J. Crivello. Polyaspartimides: Condensation of aromatic diamines and bismaleimide compounds. *Journal of Polymer Science: Polymer Chemistry Edition*, 11:1185–200, 1973.

[14] V. Sergeev, V. Shitikovand V. Pankratov. Synthesis of polymers by polycyclotrimerisation. *Russian Chemical Reviews*, 48:79, 1979.

[15] V. Pankratov, S. Vinogradova and V. Korshak. The synthesis of polycyanates by the polycyclotrimerisation of aromatic and organoelement cyanate esters. *Russian Chemical Reviews*, 46:278, 1977.

[16] Z. Aslan and Y. Alnak. Characterization of interlaminar shear strength of laminated woven E-glass / epoxy composites by four point bend shear test. *Polymer Composites*, 31:360, 2010.

[17] R. Lin, A. Lee, W. Lu and C. Lin. Catalyst effect on cure reactions in the blend of aromatic dicyanate ester and bismaleimide. *Journal of Applied Polymer Science*, 94:345-54, 2004.